

## FEDSM-ICNMM2010-' 0) ) )

### MODELING OF PARTICLES DISPERSION ON LIQUID SURFACES

**Sathishkumar Gurupatham, Bhavin Dalal, Sai Nudurupati,  
Ian S Fischer, Pushendra Singh**  
Department of Mechanical and Industrial Engineering  
New Jersey Institute of Technology  
Newark, New Jersey 07102, U.S.A.

**Daniel D. Joseph**  
Department of Aerospace Engineering  
Mechanics  
University of Minnesota  
Minneapolis, MN 55455, USA

#### ABSTRACT

When small particles (e.g., flour, pollen, etc.) come in contact with a liquid surface, they immediately disperse. The dispersion can occur so quickly that it appears explosive, especially for small particles on the surface of mobile liquids like water. This explosive-like dispersion is the consequence of capillary forces pulling particles into the interface causing them to accelerate to a relatively large velocity. The maximum velocity increases with decreasing particle size; for nanometer-sized particles (e.g., viruses and proteins), the velocity on an air-water interface can be as large as 47 m/s. We also show that particles oscillate at a relatively-high frequency about their floating equilibrium before coming to stop under viscous drag. The observed dispersion is a result of strong repulsive hydrodynamic forces that arise because of these oscillations.

#### INTRODUCTION

The following experiment can be easily performed in any reasonably well-equipped kitchen. Fill a dish partially with water, wait for a few minutes for the water to become quiescent, and then sprinkle a small amount of wheat flour or corn flour onto the water surface. The moment the flour comes in contact with the surface it quickly disperses into an approximately circular shaped region, forming a monolayer of dispersed flour particles on the surface (see figure 1). The interfacial forces that cause this sudden dispersion of flour particles are, in fact, so strong that a few milligrams of flour sprinkled onto the surface almost instantaneously covers the entire surface of the water contained in the dish. The same dynamics were observed for more viscous liquids except that the dispersion speeds were smaller.

The fluid dynamics of the attractive phase are well understood, but to our knowledge, there is no mention in the past studies of the initial violent dispersion despite the fact that this dispersion is ubiquitous, and occurs for many common liquids and particles.

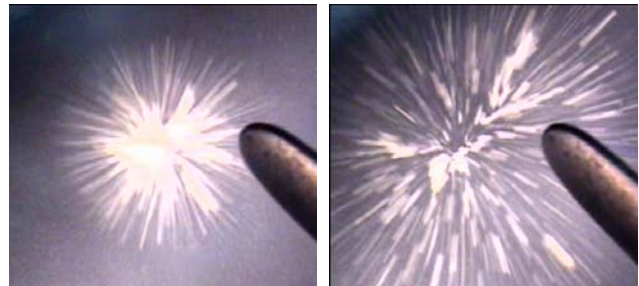


FIGURE1. Sudden dispersion of flour particles sprinkled onto water in a Petri dish.

#### RESULTS

It is shown in [1] that when small particles, e.g., flour, pollen, etc., come in contact with a liquid surface they immediately disperse. This is due to the fact that when particles come in contact with a liquid surface they are pulled inwards, towards their equilibrium position within the interface, causing them to accelerate to a relatively large velocity in the vertical direction. The observed dispersion is a result of the repulsive lateral hydrodynamic forces that arise. Furthermore, particles induce a flow on the interface that causes particles already present on the interface to move apart. These interactions between the newly-adsorbed particles and those already on the interface may alter the distribution of particles on the interface, especially when there is a continuous influx of particles to the interface.

Experiments show that when a test particle is trapped at the air-water interface, all of the nearby tracer particles on the interface (placed for flow visualization) move outward away from the test particle. The velocity of tracer particles decreases with increasing distance from the test particle. This implies that the test particle induces a flow away from itself on the interface, the strength of which decreases with increasing distance from the particle (see figure 2). Furthermore, the velocity of tracer particles was maximal shortly after the test particle came in contact with the interface and then it decreased with time. For a tracer initially at a distance of 2.05 mm from the center of the test particle, the velocity decayed to approximately zero at  $t=0.8$  s (see figure 3). The results obtained for a mixture of 60% glycerin in water were qualitatively similar except for that the velocity of tracer particles was smaller. This was expected since the viscosity of the glycerin mixture is larger than that of water and the interfacial tension is smaller.

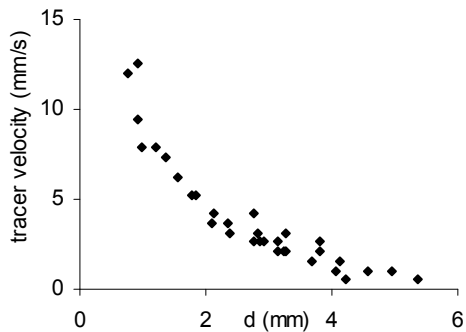


Figure 2. The velocity of tracer particles on the air-water interface is plotted as a function of the distance  $d$  from the center of a glass test particle. The velocity distribution plotted here was recorded at a time 0.033 s after the particle was trapped at the interface. The data was taken for 7 different test particles of the same approximate diameter of 850  $\mu\text{m}$ .

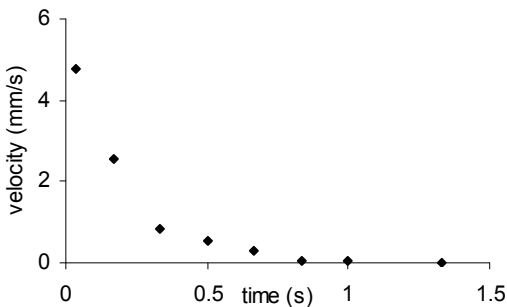


Figure 3. The velocity of a tracer particle on the air-water interface initially at a distance of 2.05 mm from a glass test particle of diameter 850  $\mu\text{m}$  is shown as a function of time. The velocity became negligibly small at  $t \sim 0.8$  s.

When two test particles were dropped together, they moved away from each other along the line joining their centers. Figure 4 shows that the separation velocity decreased with increasing time, and the velocities of the

two particles were approximately equal in magnitude. The relative velocity with which particles separated decreased with increasing initial distance between them. Furthermore, after some time, larger-sized particles reversed their direction to come back to cluster under the action of attractive lateral capillary forces that arise because of the particles' buoyant weight. The velocity with which they came back, however, was significantly smaller than the velocity with which they dispersed. Micron (less than 10  $\mu\text{m}$ ) sized particles for which lateral capillary forces are negligible, however, remained dispersed.

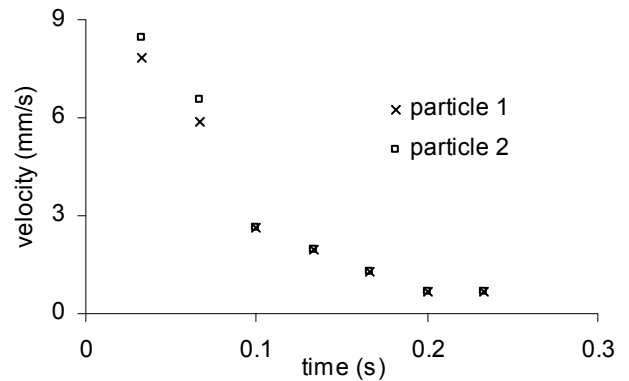


Figure 4. The velocity of two glass particles of diameter 850  $\mu\text{m}$  dropped simultaneously onto the air-water interface is shown as a function of time. The initial distance between the particles was 1.21 mm. After becoming trapped in the interface, they moved apart approximately along the line joining their centers. The magnitude of the velocities of the two particles was approximately equal.

This behavior of particles was also seen in direct numerical simulations in which the particle centers were initially at a height of  $0.95R$  above the undeformed interface. The particles were pulled downwards by the vertical capillary forces leading to vertical oscillations. The amplitude of the oscillations decreased with increasing time. The particles also moved apart as shown in figure 5.

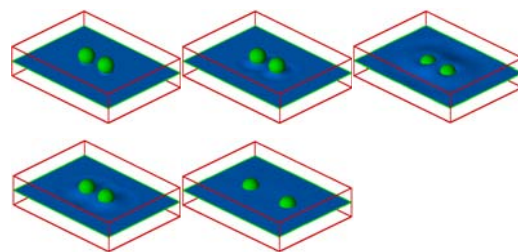


Figure 5. Direct numerical simulation of the motion of two particles released above their equilibrium height in the interface.

The main driving forces for the motion of a particle normal to the interface (after it comes in contact with the interface) are the vertical capillary force and the particle's

buoyant weight. The viscous drag resists the particle's motion. The acceleration of the particle under the action of these forces can be written as:

$$m \frac{dV}{dt} = F_{st} + F_D + F_g, \quad (1)$$

where  $m$  is the effective mass of the particle which includes the added mass contribution,  $V$  is the particle velocity,  $F_{st}$  is the vertical capillary force,  $F_D$  is the drag, and  $F_g$  is the gravity force.

The right hand side of the above equation was approximated in [1] by assuming that the particle is spherical, the contact angle is equal to its equilibrium value, the drag force is given by the Stokes formula, and the buoyancy force depends on the particle's vertical position, to obtain

$$m \frac{dV}{dt} = -2\pi(R \sin \theta_c) \gamma_{12} \sin(\theta_c + \alpha) - 6\pi R \mu V \zeta(s) + Q(\rho_p - \rho_c)g. \quad (2)$$

Here  $\zeta(s)$  is a factor that accounts for the dependence of the drag on the fraction  $s$  of the particle that is immersed in the lower and upper fluids and on the viscosities of the fluids involved,  $Q$  is the particle volume,  $\rho_c$  is the effective fluid density which changes with  $s$  while the particle moves normal to the interface, and  $\rho_p$  is the particle density.

Equation (2) was solved numerically in [1] to obtain the particle's position as a function of time. The obtained solution was qualitatively similar to that obtained using the DNS approach (see figure 1). Equation (2) can be linearized about the particle's equilibrium position to show that it is equivalent to a spring-dashpot system. Assuming that  $\alpha = \frac{\pi}{2}$ ,  $\theta_c = \frac{\pi}{2}$  and  $\zeta(s) = 1/2$ , after linearization, we obtain

$$\frac{4}{3} R^3 \rho_p \frac{d^2 Z}{dt^2} + 3R\mu \frac{dZ}{dt} + 2\gamma_{12} Z + R^2(\rho_p - \rho_c)g Z = 0, \quad (3)$$

where  $Z$  is the particle's position. The solution of the above ordinary differential equation can be written as:

$$Z = Z_0 e^{kt}, \quad (4)$$

where  $k = \frac{-3R\mu \pm \sqrt{D}}{\frac{8}{3} R^3 \rho_p}$  and

$$D = 9R^2 \mu^2 - \frac{16}{3} R^3 \rho_p (2\gamma_{12} + R^2(\rho_p - \rho_c)g). \quad (5)$$

solution depends on the sign of  $D$ . If the sign is positive, then  $k$  is real and negative for both of the roots. In this case, the solution decays exponentially with time to zero. This is expected to be the case when the fluid viscosity is sufficiently large. If the sign of  $D$  is negative, then  $k$  is complex and the solution is oscillatory. In this case, the frequency of the oscillation is given by

$$\omega = \frac{3\sqrt{-9R^2 \mu^2 + \frac{16}{3} R^3 \rho_p (2\gamma_{12} + R^2(\rho_p - \rho_c)g)}}{16\pi R^3 \rho_p}. \quad (5)$$

The real parts of both roots are negative and so both of the solutions decay exponentially to zero. The frequency of oscillation ( $\omega$ ) in Hz is plotted as a function of the particle radius in figure 2; it increases with decreasing particle radius.

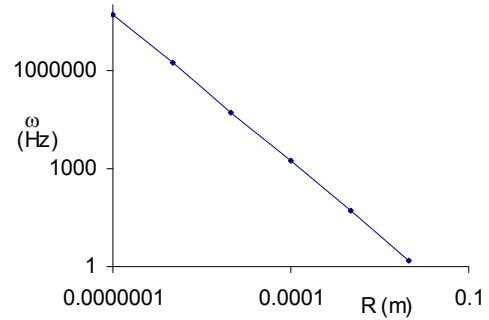


Figure 6. The frequency ( $\omega$ ) of oscillation of the solution given by equation (16) is plotted as a function of the particle radius. The parameter values were assumed to be:  $\mu = 0.001$  Pa.s,  $\rho_p = 1000.0$  kg/m<sup>3</sup>,  $\rho_p - \rho_c = 0.1$  kg/m<sup>3</sup> and  $\gamma_{12} = 0.07$  N/m.

The particle velocity when it reaches its equilibrium position for the *first* time can be obtained by integrating Eq(2)

$$V = \frac{-\frac{9}{4}\mu + \sqrt{\frac{81}{16}\mu^2 + 4R\rho_p \left( \frac{3}{2}\gamma + 2R^2(\rho_p - \rho_c)g \right)}}{2R\rho_p}. \quad (5)$$

The above equation implies that the maximum velocity attained by a particle increases with decreasing particle radius (see figure 3). For example, a particle of diameter 200  $\mu$ m (which is roughly the size of a sand particle) can accelerate to a velocity of the order of 1 m/s at the water surface, and a particle of diameter 10 nm, which is roughly the size of a virus or a protein molecule, to a velocity of ~40 m/s. In the limit of  $R$  approaching zero, the velocity is given by

$$V = \frac{2\gamma}{3\mu}. \quad (6)$$

This is the maximum velocity that can be attained by a particle under the action of the vertical capillary force, which for the air-water interface is 46.7 m/s.

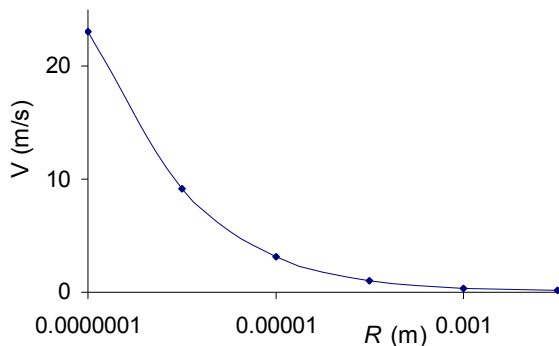


Figure 7. The velocity of a spherical particle normal to the interface given by equation (5) is plotted as a function of the particle radius. The parameter values are the same as in figure 2.

## Conclusions

It is shown that when a particle comes in contact with a liquid surface it is pulled into the interface towards its equilibrium height by the vertical capillary force and that during this process the particle can accelerate to a relatively large velocity normal to the interface. For example, a particle of radius 100  $\mu\text{m}$  sprinkled onto the water surface may attain a velocity of the order of 1 m/s. The maximum velocity on an air-water interface, which increases with decreasing particle size, can be as large as  $\sim 47$  m/s. It is also shown that a particle being adsorbed oscillates about its equilibrium height before coming to rest under viscous drag. These oscillations of the particle cause the fluid around it to move away, which in our experiments was measured using smaller tracer particles that were present on the liquid surface.

When two or more particles are dropped simultaneously onto the surface their motion in the direction normal to the interface (and to the line joining their centers) gives rise to the strong repulsive hydrodynamic forces which cause them to move apart. The velocity with which particles move apart increases with an increasing number of particles. Also, smaller-sized particles disperse more readily because the importance of interfacial forces increases with decreasing particle radius. An analysis of the particle's equation for the vertical motion is used to determine the dependence of the velocity on the factors such as the fluid viscosity, the change in the interfacial energy due to the adsorption of the particle, the particle radius, and the buoyant weight. The viscous drag causes the oscillatory motion of particles about their equilibrium heights to decay with time, and thus the repulsive hydrodynamic forces that arise because of this motion also decrease with time. As

a result, after reaching a maximum value, the velocity with which particles move apart decreases with time. Furthermore, if the buoyant weight of particles is not negligible, e.g., 200  $\mu\text{m}$  sized sand particles used in Figure 1, they also experience attractive lateral capillary forces that arise because of the deformation of the interface. Although these attractive lateral forces are relatively weaker, after the repulsive hydrodynamic forces become smaller they cause particles to come back to cluster. However, the velocity with which particles come back to cluster is much smaller. Micron- and nano-sized particles, on the other hand, remain dispersed since for them the attractive capillary forces are negligible.

## REFERENCES

1. Chan, D.Y.C., Henry, J.D., Jr. and White, L.R. (1981) The interaction of colloidal particles collected at the fluid interface, *J. Colloid Interface Sci.* **79**, 410.
2. Fortes, M.A. (1982) Attraction and repulsion of floating particles, *Can. J. Chem.* **60**, 2889.
3. Katoh, K., Fujita, H. and Imazu, E. (1992) Motion of a particle floating on a liquid meniscus surface, *J. Fluids Engrg.*, **114**, 411.
4. Nicolson, M.M. (1949) The interaction between floating particles, *Proc. Cambridge Philosophical Soc.* **45**, 288.
5. Princen, H.M. (1969) Equilibrium shape of interfaces, drops and bubbles. Rigid and deformable particles at interfaces, *Surface and Colloid Science*, E. Matijevic, ed., Interscience, New York, 2, 1.
6. Rapacchietta A.V. and Neumann, A.W. (1977) Force and free-energy analyses of small particles at fluid interfaces: II. Spheres, *J. Colloid and Interface Sci.*, **59**(3), 555-567.
7. Singh, P. and Joseph, D.D. (2005) Fluid dynamics of Floating particles, *J. of Fluid Mech.*, **530**, 31.
8. Pillapakam, S.B. and Singh, P. (2001) A Level Set Method for computing solutions to viscoelastic two-phase flow, *J. Computational Physics*, **174**, 552-578.
9. Singh, P., Hesla, T.I. and Joseph, D.D. (2003) A Modified Distributed Lagrange Multiplier/Fictitious Domain Method for Particulate Flows with Collisions, *Int. J. of Multiphase Flows*, **29**, 495-509.
10. Singh, P., Joseph, D.D., Hesla, T.I., Glowinski, R. and Pan, T.W. (2000) A distributed Lagrange multiplier/fictitious domain method for viscoelastic particulate flows, *J. Non-Newtonian Fluid Mech.* **91**, 165.
11. P. Singh, D.D. Joseph, S.K. Gurupatham, B. Dalal and S. Nudurupati, *Proceedings of the National Academy of Sciences U.S.A.*, 106, 19761-19764, 2009.